Intracellular metabolite β-glucosylceramide is an endogenous Mincle ligand possessing immunostimulatory activity

Masahiro Nagata[a], Yoshihiro Izumi[b], Eri Ishikawa[a], Ryoko Kiyotake[a], Rieko Doi[a], Satoru Iwai[a], Zakaria Omahdi[a], Toshiyuki Yamaji[c], Tomofumi Miyamoto[d], Takeshi Bamba[b], and Sho Yamasaki[a,e,f,1]

[a]Division of Molecular Immunology, Medical Institute of Bioregulation, Kyushu University, Fukuoka 812-8582, Japan; [b]Division of Metabolomics, Medical Institute of Bioregulation, Kyushu University, Fukuoka 812-8582, Japan; [c]Department of Biochemistry and Cell Biology, National Institute of Infectious Diseases, Shinjuku-ku, Tokyo 162-8640, Japan; [d]Department of Natural Products Chemistry, Graduate School of Pharmaceutical Sciences, Kyushu University, Fukuoka 812-8582, Japan; [e]Department of Molecular Immunology, Research Institute for Microbial Diseases, Osaka University, Suita, 565-0871, Japan; and [f]Division of Molecular Immunology, Medical Mycology Research Center, Chiba University, Chiba 260-8673, Japan

Sensing and reacting to tissue damage is a fundamental function of immune systems. Macrophage inducible C-type lectin (Mincle) is an activating C-type lectin receptor that senses damaged cells. Notably, Mincle also recognizes glycolipid ligands on pathogens. To elucidate endogenous glycolipids ligands derived from damaged cells, we fractionated supernatants from damaged cells and identified a lipophilic component that activates reporter cells expressing Mincle. Mass spectrometry and NMR spectroscopy identified the component structure as β-glucosylceramide (GlcCer), which is a ubiquitous intracellular metabolite. Synthetic β-GlcCer activated myeloid cells and induced production of inflammatory cytokines; this production was abrogated in Mincle-deficient cells. Sterile inflammation induced by excessive cell death in the thymus was exacerbated by hematopoietic-specific deletion of degrading enzyme of β-GlcCer (β-glucosylceramidase, GBA1). However, this enhanced inflammation was ameliorated in a Mincle-deficient background. GBA1-deficient dendritic cells (DCs) in which β-GlcCer accumulates triggered antigen-specific T-cell responses more efficiently than WT DCs, whereas these responses were compromised in DCs from GBA1 × Mincle double-deficient mice. These results suggest that β-GlcCer is an endogenous ligand for Mincle and possesses immunostimulatory activity.

C-type lectin receptors | glycolipids | ceramides | inflammation | Gaucher disease

Excessive or deregulated cell death caused by noninfectious insults often leads to inflammatory responses through the release and exposure of intracellular components. These components activate myeloid cells to initiate innate and acquired immune responses through pattern recognition receptors, such as Toll-like receptors (TLRs), Nod-like receptors, RIG-I-like receptors, and C-type lectin receptors (CLRs) (1–4).

Macrophage inducible C-type lectin (Mincle, also called Clec4e) is an activating receptor that senses dead cells (5). In addition, Mincle recognizes pathogens, including mycobacteria through bipolar glycolipids, such as trehalose 6,6′-dimycolate (TDM), which act as pathogen-associated molecular patterns (6–8). Structural analysis of the Mincle protein has revealed how its unique ligand-binding site is suitable for glycolipid recognition (9–12). Hence, we hypothesized that Mincle may recognize endogenous glycolipids released from damaged cells.

Glycosphingolipids (GSLs) are cell-bound bipolar glycolipids involved in a wide variety of fundamental biological processes and cell-specific functions in mammals. GSLs possess various saccharides and a ceramide in which fatty acids (FA) are attached to the platform sphingosine. One such ceramide is β-glucosylceramide (β-GlcCer), which is the first intermediate in the synthesis of a large family of GSLs. In healthy individuals, β-GlcCer is thought to be localized in the endoplasmic reticulum/Golgi apparatus (13–15), and the intracellular level of β-GlcCer is tightly

regulated by a balance between biosynthesis and degradation to maintain tissue homeostasis (16–18). Therefore, an elevation in the levels of β-GlcCer in the extracellular milieu might signal massive cell death or tissue damage. In fact, a homozygous mutation in human β-glucocerebrosidase (GBA1), a crucial enzyme degrading β-GlcCer, leads to Gaucher disease because of a reduction in enzyme activity that causes accumulation of β-GlcCer (19). Gaucher disease is characterized by systemic inflammation, which presents hepatosplenomegaly or neurodegeneration (20–24). However, the molecular mechanisms that link excessive β-GlcCer to inflammatory responses are not yet understood. Furthermore, the immune receptor that directly recognizes β-GlcCer is unknown and it is unclear whether β-GlcCer possesses immunostimulatory potential.

In this study, we purified an endogenous Mincle ligand from the supernatants of damaged cells and used structural analysis to identify the ligand as β-GlcCer. Using GBA1-deficient and Mincle-deficient mice, we show that in vivo immune responses associated with β-GlcCer accumulation are compromised in a Mincle-deficient background.

Results

Purification of Endogenous Mincle Ligand. We previously reported that Mincle-expressing cells are spontaneously activated in the

Significance

Sensing tissue damage is a crucial function of pattern recognition receptors (PRRs). However, endogenous ligand recognition by PRRs is not well documented. Macrophage inducible C-type lectin (Mincle) is a PRR that recognizes both pathogens and damaged cells. In this study, we isolated endogenous glycolipids derived from damaged cells and identified a ubiquitous intracellular metabolite, β-glucosylceramide (GlcCer), as a Mincle ligand. β-GlcCer induced inflammatory and acquired immune responses via Mincle on myeloid cells. Accumulation of β-GlcCer leads to Gaucher disease, a disorder characterized mainly by systemic inflammation. In a Gaucher model in which mice are deficient in the β-GlcCer–degrading enzyme, further deletion of the Mincle gene attenuated inflammatory responses. These results suggest that β-GlcCer is an endogenous Mincle ligand and acts as an immunostimulatory factor upon cell damage.

presence of dying cells (5). Therefore, we set out to investigate whether Mincle recognizes any endogenous glycolipids associated with cell damage. To this end, we collected the culture supernatants of damaged cells and conducted solvent-based extraction of lipophilic components using chloroform:methanol. The soluble extract was separated into 30 fractions by HPLC and the ligand activity of each fraction was assessed using reporter cells expressing Mincle. We detected ligand activity that peaked in fraction **4** from cell supernatants but not from medium alone (Fig. 1 *A* and *B*). Thin-layer chromatography (TLC) analysis
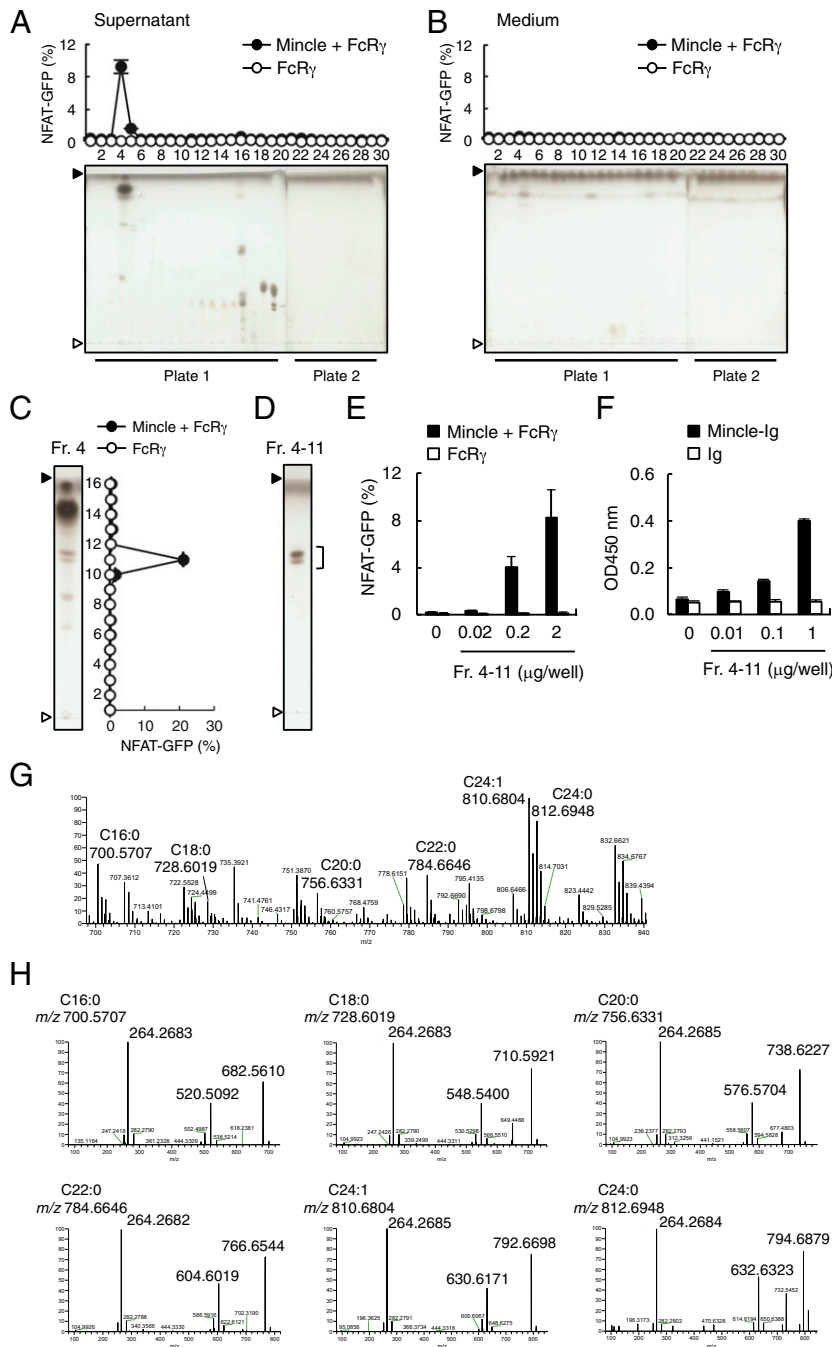

Fig. 1. Identification of Mincle ligands in the culture supernatants of dead cells. (*A* and *B*) NFAT-GFP reporter cells expressing Mincle + FcRγ or FcRγ only were stimulated with HPLC-separated lipid fractions from supernatants of dead reporter cells (*A*) or medium only (*B*) for 18 h. Induction of NFAT-GFP was assessed by flow cytometry. Each fraction was analyzed by HPTLC (plate 1: fraction 1–20; plate 2: fraction 21–30) developed with chloroform/methanol/water (65:25:4, vol/vol/vol). The HPTLC plates were stained with copper acetate-phosphoric acid. Prior to spotting the fractions, two lines for the origin and the solvent front were marked on the plate with a soft pencil. Open and closed arrowheads denote the origin and solvent fronts, respectively. (*C*) Reporter cell activity of HPTLC-separated subfractions of fraction (Fr.) **4** shown in *A*. (*D*) Fr. **4-11** in *C* was visualized by HPTLC followed by copper acetate-phosphoric acid staining. (*E*) Reporter cells were stimulated with the indicated amount of Fr. **4-11**. (*F*) Binding assay of Ig control (Ig) and Mincle-Ig fusion with the indicated amount of Fr. **4-11**. (*G*) Full-scan MS spectra of Fr. **4-11** in the positive ion mode. (*H*) MS/MS spectra of each glycosylceramide; C16:0 (*m/z* 700.5707), C18:0 (*m/z* 728.6019), C20:0 (*m/z* 756.6331), C22:0 (*m/z* 784.6646), C24:1 (*m/z* 810.6804) and C24:0 (*m/z* 812.6948) in the positive-ion mode. Data are presented as mean ± SD of duplicate (*A–C, E*) and triplicate (*F*) assays.

Table 1. List of glycosylceramides detected in the culture supernatant of dead cells by ESI-Q-Orbitrap-MS

Glycosylceramide	Molecular formula	Precursor ion (M+H)$^+$				Characteristic product ions				
		Theoretical (m/z)	Observed (m/z)	Error (ppm)	Observed (m/z)*	Error (ppm)	Observed (m/z)†	Error (ppm)	Observed (m/z)‡	Error (ppm)
(d18:1/12:0)	$C_{36}H_{69}NO_8$	644.5101	ND	—	—	—	—	—	—	—
(d18:1/13:0)	$C_{37}H_{71}NO_8$	658.5258	ND	—	—	—	—	—	—	—
(d18:1/14:1)	$C_{38}H_{71}NO_8$	670.5258	ND	—	—	—	—	—	—	—
(d18:1/14:0)	$C_{38}H_{73}NO_8$	672.5414	ND	—	—	—	—	—	—	—
(d18:1/15:0)	$C_{39}H_{75}NO_8$	686.5571	ND	—	—	—	—	—	—	—
(d18:1/16:1)	$C_{40}H_{75}NO_8$	698.5571	ND	—	—	—	—	—	—	—
(d18:1/16:0)	**$C_{40}H_{77}NO_8$**	**700.5727**	**700.5707**	**2.9**	**264.2683**	**3.0**	**520.5092**	**0.3**	**682.5610**	**1.7**
(d18:1/17:0)	$C_{41}H_{79}NO_8$	714.5884	ND	—	—	—	—	—	—	—
(d18:1/18:4)	$C_{42}H_{73}NO_8$	720.5414	ND	—	—	—	—	—	—	—
(d18:1/18:3)	$C_{42}H_{75}NO_8$	722.5571	ND	—	—	—	—	—	—	—
(d18:1/18:2)	$C_{42}H_{77}NO_8$	724.5727	ND	—	—	—	—	—	—	—
(d18:1/18:1)	$C_{42}H_{79}NO_8$	726.5884	ND	—	—	—	—	—	—	—
(d18:1/18:0)	**$C_{42}H_{81}NO_8$**	**728.6040**	**728.6019**	**2.9**	**264.2683**	**3.0**	**548.5400**	**1.2**	**710.5921**	**1.9**
(d18:1/19:0)	$C_{43}H_{83}NO_8$	742.6197	ND	—	—	—	—	—	—	—
(d18:1/20:5)	$C_{44}H_{75}NO_8$	746.5571	ND	—	—	—	—	—	—	—
(d18:1/20:4)	$C_{44}H_{77}NO_8$	748.5727	ND	—	—	—	—	—	—	—
(d18:1/20:3)	$C_{44}H_{79}NO_8$	750.5884	ND	—	—	—	—	—	—	—
(d18:1/20:2)	$C_{44}H_{81}NO_8$	752.6040	ND	—	—	—	—	—	—	—
(d18:1/20:1)	$C_{44}H_{83}NO_8$	754.6197	ND	—	—	—	—	—	—	—
(d18:1/20:0)	**$C_{44}H_{85}NO_8$**	**756.6353**	**756.6331**	**3.0**	**264.2685**	**2.3**	**576.5704**	**2.7**	**738.6227**	**2.8**
(d18:1/21:0)	$C_{45}H_{87}NO_8$	770.6510	ND	—	—	—	—	—	—	—
(d18:1/22:6)	$C_{46}H_{77}NO_8$	772.5727	ND	—	—	—	—	—	—	—
(d18:1/22:5)	$C_{46}H_{79}NO_8$	774.5884	ND	—	—	—	—	—	—	—
(d18:1/22:4)	$C_{46}H_{81}NO_8$	776.6040	ND	—	—	—	—	—	—	—
(d18:1/22:3)	$C_{46}H_{83}NO_8$	778.6197	ND	—	—	—	—	—	—	—
(d18:1/22:2)	$C_{46}H_{85}NO_8$	780.6353	ND	—	—	—	—	—	—	—
(d18:1/22:1)	$C_{46}H_{87}NO_8$	782.6510	ND	—	—	—	—	—	—	—
(d18:1/22:0)	**$C_{46}H_{89}NO_8$**	**784.6666**	**784.6646**	**2.6**	**264.2682**	**3.4**	**604.6019**	**2.2**	**766.6544**	**2.2**
(d18:1/23:0)	$C_{47}H_{91}NO_8$	798.6823	ND	—	—	—	—	—	—	—
(d18:1/24:2)	$C_{48}H_{89}NO_8$	808.6666	ND	—	—	—	—	—	—	—
(d18:1/24:1)	**$C_{48}H_{91}NO_8$**	**810.6823**	**810.6804**	**2.3**	**264.2685**	**2.3**	**630.6171**	**2.9**	**792.6698**	**2.4**
(d18:1/24:0)	**$C_{48}H_{93}NO_8$**	**812.6979**	**812.6948**	**3.9**	**264.2684**	**2.6**	**632.6323**	**3.6**	**794.6879**	**0.7**
(d18:1/25:0)	$C_{49}H_{95}NO_8$	826.7136	ND	—	—	—	—	—	—	—
(d18:1/26:0)	$C_{50}H_{97}NO_8$	840.7292	ND	—	—	—	—	—	—	—
(d18:1/27:0)	$C_{51}H_{99}NO_8$	854.7449	ND	—	—	—	—	—	—	—
(d18:1/28:0)	$C_{52}H_{101}NO_8$	868.7605	ND	—	—	—	—	—	—	—

The assignment of chemical composition is based on accurate mass measurements, comparison of isotopic patterns, and tandem MS fragmentation patterns. The glycosylceramides detected in the culture supernatant are shown in bold characters.
*The conjugated aziridine ion of d18:1/n-FA-ceramide.
†The loss of glycosyl residue.
‡The loss of water (dehydration).

demonstrated that this fraction contains several compounds as visualized by copper acetate staining. Fraction **4** was further characterized by means of high-performance TLC (HPTLC) and separated into 16 subfractions. Because fraction **4-11** contained the unique peak of activity (Fig. 1C), we collected this active spot by HPTLC (Fig. 1D) and confirmed its recognition by reporter cells (Fig. 1E) and Mincle-Ig binding (Fig. 1F).

We next analyzed fraction **4-11** by electron spray ionization-quadrupole Orbitrap mass spectrometry (ESI-Q-Orbitrap-MS) (25). As shown in Fig. 1 G and H, the positive full-scanning MS and MS/MS (MS^2) spectra of fraction **4-11** showed at m/z 700.5707 (C16:0), 728.6019 (C18:0), 756.6331 (C20:0), 784.6646 (C22:0), 810.6804 (C24:1), and 812.6948 (C24:0) [M + H]$^+$ that this fraction contained six monoglycosyl sphingolipid species (Fig. 1G). Indeed, we observed the characteristic product ions of glycosylceramide. For example, MS^2 spectra arising from the dissociation of the precursor ion at m/z 700.5707 represent mainly the conjugated aziridine ion of d18:1/n-FA-ceramide (m/z 264.2683) (26), the loss of a glycosyl residue (m/z 520.5092), and the dehydrated glyco-

sylceramide (m/z 682.5610) (Fig. 1H). By matching these mass data against a public database (27), these glycosphingolipids appear to be either β-GlcCer or β-galactosylceramide (β-GalCer). Given that β-GlcCer is an abundant GSL in various tissues, we speculated that these six species of GlcCer are potential candidates for endogenous Mincle ligands (Table 1).

Structural Analyses of Endogenous Mincle Ligand. To investigate whether the putative Mincle ligands are synthesized upon damage to cells or are constitutively present within cells, we assessed the ligand activity of extracts from living cells. An active fraction, which corresponded to that of the supernatants from damaged cells (Fig. 1C), was also detected in extracts of living cells (Fig. 2A, Left). However, the amount of active component was decreased in dead cells (Fig. 2A, Right), indicating that the ligand exists constitutively in living cells and is presumably released upon cell damage. To perform detailed structural analyses, we collected a large amount of active fraction from living cells (Fig. 2B) and confirmed by MS

that the species contained in this fraction were identical to those purified from the supernatants from damaged cells (Fig. S1).

To determine the core structure, we used NMR analyses, including extensive 2D NMR experiments (COSY, TOCSY, NOESY, HSQC, HMBC). The ^{1}H- and ^{13}C-NMR spectra of this fraction showed the typical signal of a β-GlcCer structure composed by a sphingosine and β-glucopyranose (Fig. S2 *A and B*) and these NMR chemical shifts were identical to previous data, which reported the GlcCer core structure (28, 29). The signals of ^{1}H-NMR showed terminal methyl protons [δ$_H$ 0.89 (6H, t, 6.7)], methylene protons (δ$_H$ 1.27), methylene protons on the carbonyl group of the amide linkage [δ$_H$ 2.17 (2H, t, 7.9)], the characteristic double bond in sphingosine [δ$_H$ 5.45 (dd, 7.6, 15.3), δ$_H$ 5.70 (dt, 7.9, 15.3)], and the anomeric proton of β-glucopyranoside [δ$_H$ 4.29 (d, 7.9)]. The signals of ^{13}C-NMR exhibited: a terminal methyl signal at δ$_C$ 14.2 (q); core carbon in the sphingosine signal at δ$_C$ 69.1 (t), δ$_C$ 53.6 (d), δ$_C$ 72.2 (d); double bond in the sphingosine at δ$_C$ 129.6 (d), δ$_C$ 134.9 (d); carbon signal in the carbonyl group of the amide linkage at δ$_C$ 175.3 (s); and an anomeric carbon signal at δ$_C$ 103.4 (d). These MS and NMR results support the idea that these active components are β-GlcCers.

We further analyzed the structure of the FA and long-chain base by methanolysis followed by GC-MS analysis: results showed that the active fraction contains five saturated FA methyl esters (FAMEs) (16:0, 18:0, 20:0, 22:0, and 24:0) and one unsaturated FAME (24:1) (Fig. S2C). The olefinic proton and carbon signals were observed at δ$_H$ 5.35 [0.75H, t, 4.5), δ$_C$ 130.2 (d)] (Fig. S2 *A and B*) and the allylic carbon signals were assigned to δ$_C$ 27.4 (t) (C14, 17) (Fig. S2*A*). These chemical shifts revealed the geometry of this double bond to be Z (30). We next determined the position of the double bond. After RuCl-oxidation followed by CH$_2$N$_2$-imidazole treatment, the peak corresponding to the C24:1-methylated FA was completely abolished, leaving only C15:0-dicarboxylic acid methyl ester to be detected as the product of RuCl-oxidation and CH$_2$N$_2$-treated C24:1 FA (Fig. S2 *D and E*). This finding suggested that the position of the double bond was C15. We also confirmed the presence of the glucose moiety by GC-MS following methanolysis and trimethylsilyl (TMS)-imidazole treatment. C18 sphingosine and glucose were identified by mass spectra and comparison with a standard control (Fig. S2 *F and G*). Taken together, these analyses indicated that the active fraction consists of five saturated FAs (16:0, 18:0, 20:0, 22:0 and 24:0), one unsaturated FA [24:1 (15Z)], and a sphingosine [(2S, 3R, 4E)-2-amino-4-octadecene-1,3-diol] (Fig. 2C).

Given that it is a common GSL among mammals, we also analyzed human reporter cells expressing Mincle for β-GlcCer. Consistent with the previous findings in murine cells (5), when the HEK293-based NF-κB reporter cells were cultured alone without medium change for an extended time, cells became damaged and Mincle reporter activity was gradually induced (Fig. 2D). Within the supernatant, we also detected an active spot by HPTLC corresponding to β-GlcCer (Fig. S3A). To determine whether this activation is indeed mediated by β-GlcCer, D-*threo*-1-phenyl-2-decanoylamino-3-morpholino-1-propanol (D-PDMP), an inhibitor of the UDP-glucose ceramide synthase (UGCG) (31), was added during the culture period. D-PDMP selectively blocked β-GlcCer synthesis (Fig. 2E) and Mincle reporter activity (Fig. 2F), suggesting that β-GlcCer represents a key factor mediating Mincle activation by damaged cells.

Mincle Recognizes Synthetic β-GlcCer. To confirm that the activity of β-GlcCer is not a result of minor contaminants, we examined the ligand activity of synthetic β-GlcCer (C24:1). Indeed, the synthetic compound potently activated reporter cells expressing murine and human Mincle (Fig. 3A and Fig. S3B). This activity was specific for Mincle, as other related CLRs—such as MCL (Clec4d), Dectin-2 (Clec4n), and DCAR (Clec4b1)—did not
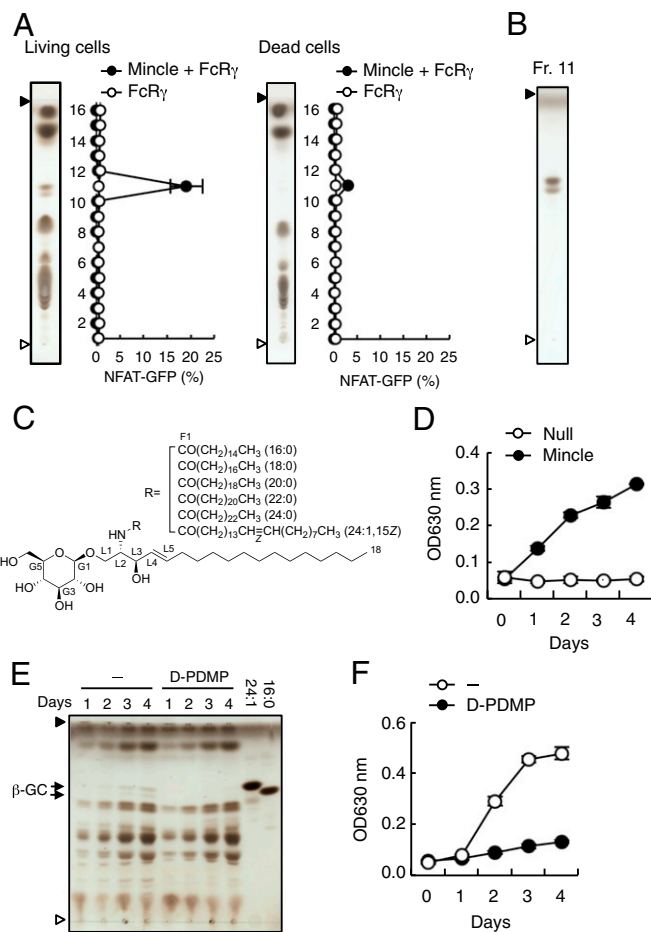
Fig. 2. The Mincle endogenous ligand β-GlcCer is present in living cells and released upon cell death. (A) Mincle + FcRγ-expressing NFAT-GFP reporter cells were stimulated with HPTLC-separated lipid fractions from living (*Left*) or dead (*Right*) cells. Each fraction was analyzed by HPTLC as described above and GFP expression was assessed by flow cytometry. Open and closed arrowheads denote the origin and solvent fronts, respectively. (B) Fr. **11** in A was visualized by HPTLC followed by copper acetate-phosphoric acid staining. (C) Molecular structure of β-GlcCer and the different acyl chains of its derivatives. (D) SEAP reporter assay using HEK293-based NF-κB reporter cells expressing Mincle after culturing for the indicated number of days in the absence of exogenous stimulation. (E and F) NF-κB reporter cells expressing Mincle were cultured in the presence or absence of 20 μM D-PDMP for the indicated number of days. The lipid composition of these cells was analyzed by HPTLC and compared with the 24:1 and 16:0 β-GlcCer derivatives (E). Arrows indicated β-GlcCer (β-GC). The SEAP reporter assay is shown in F. Data are presented as mean ± SD of duplicate (A) and triplicate (D and F) assays.

recognize β-GlcCer (Fig. 3B). In addition to NF-AT, an NF-κB reporter gene was also activated by synthetic β-GlcCer through Mincle to levels comparable to those induced by a known ligand TDM (Fig. 3C).

Ceramide and lactosylceramide (LacCer) are upstream and downstream metabolites of β-GlcCer, respectively; however, neither of these lipids possessed ligand activity (Fig. 3D). Furthermore, β-GalCer, another downstream intermediate to sulfatides and GM4, had no activity (Fig. 3D). Thus, Mincle selectively recognizes a particular intermediate in the ceramide metabolic pathway. This finding suggests that a ceramide may require a terminal glucose, not galactose, to act as ligand.

We next tested the roles of N-acyl chain composition and length for Mincle ligand activity. The synthetic version of three of the major β-GlcCer components (C16:0, C18:0, and C24:1) were compared in reporter cell assays. Although all species possessed substantial ligand

activity, β-GlcCer C16:0 and C18:0 were less effective than C24:1 (Fig. 3E). Thus, a β-GlcCer bearing an unsaturated long chain, C24:1, appears to possess the most potent activity.

β-GlcCer Activates Myeloid Cells Through Mincle. What is the contribution of Mincle as a β-GlcCer receptor expressed in myeloid cells? β-GlcCer 24:1 treatment of bone marrow dendritic cells (BMDCs) induced the secretion of TNF and MIP-2, whereas in Mincle$^{-/-}$ BMDCs secretion of these cytokines was significantly decreased (Fig. 3F). Consistent with these results, β-GlcCer–induced production of TNF and MIP-2 was dependent on a

downstream adaptor for immunereceptor tyrosine-based activation motif (ITAM) signaling (CARD9) but not for TLR signaling (MyD88) (Fig. 3G). β-GlcCer also induced the up-regulation of surface expression of costimulatory molecules, such as CD40, CD80, CD86, and MHC class II in a Mincle-dependent manner (Fig. 3H). We conclude from these results that Mincle is the major receptor mediating β-GlcCer–induced myeloid cell activation.

β-GlcCer Promotes T-Cell Responses via Antigen-Presenting Cells. We next analyzed the effect of β-GlcCer on T-cell priming by antigen-presenting cells (APCs). To this end, ovalbumin (OVA)-specific
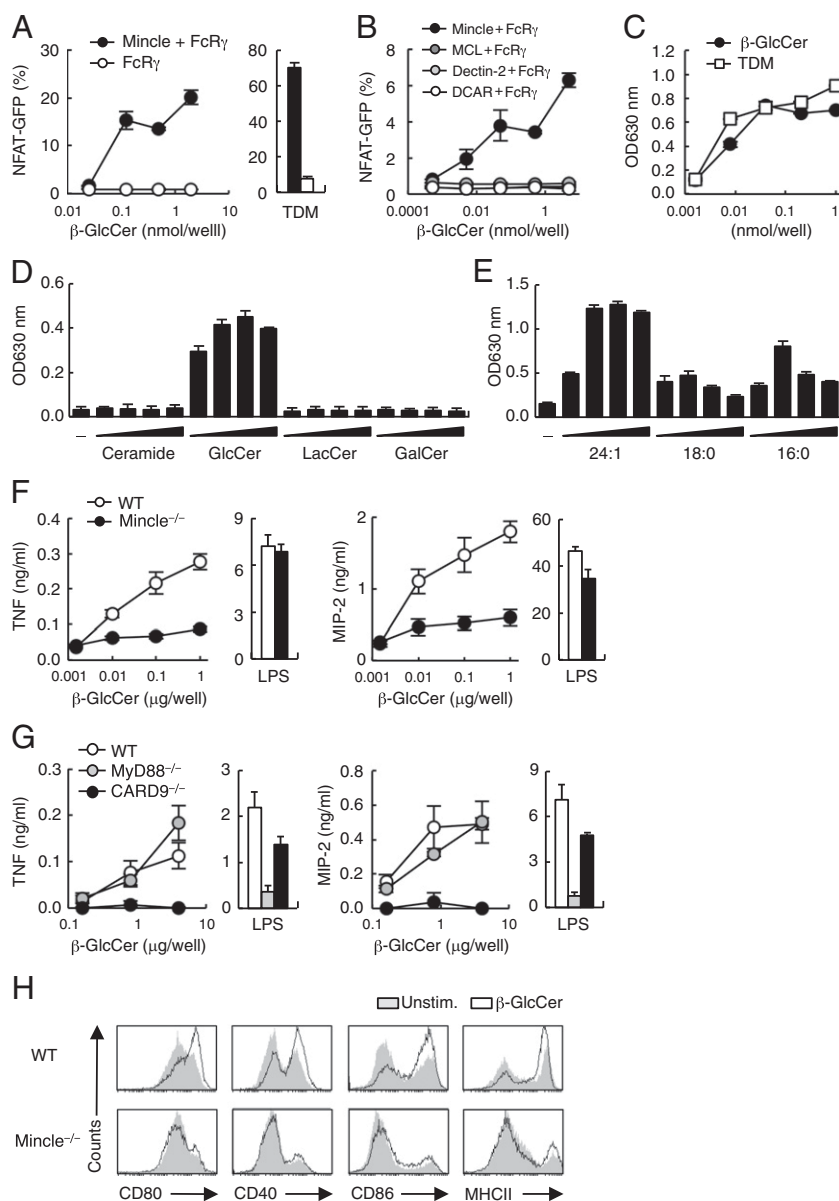

Fig. 3. Specific recognition of synthetic β-GlcCer by Mincle. (A) NFAT-GFP reporter cells expressing Mincle + FcRγ or FcRγ only were stimulated with increasing amounts of 24:1 β-GlcCer or 0.3 nmol per well TDM. (B) NFAT-GFP reporter cells expressing Mincle, MCL, Dectin-2 or DCAR were stimulated with the indicated concentrations of 24:1 β-GlcCer. (C) Mincle-expressing NF-κB reporter cells were stimulated with the indicated concentrations of 24:1 β-GlcCer or TDM. SEAP levels in culture supernatants were measured after 24 h. (D) NF-κB reporter cells were stimulated by ceramide, 24:1 β-GlcCer, LacCer, or β-GalCer at 0.016, 0.08, 0.4, 2 μg per well and reporter activity was determined. (E) NF-κB reporter cells were stimulated by β-GlcCer derivatives (24:1, 18:0, or 16:0) at 0.008, 0.04, 0.2, 1 nmol per well and reporter activity was determined. (F) WT and Mincle$^{-/-}$ BMDCs were stimulated with 24:1 β-GlcCer or 10 ng/mL LPS for 1 d. Concentrations of TNF (Left) and MIP-2 (Right) in the supernatants were measured by ELISA. (G) TNF (Left) and MIP-2 (Right) production from WT, MyD88$^{-/-}$ and CARD9$^{-/-}$ BMDCs stimulated with the indicated amounts of 24:1 β-GlcCer or 10 ng/mL LPS. (H) Surface expression levels of CD80, CD40, CD86, and MHC class II on WT and Mincle$^{-/-}$ BMDCs stimulated with 24:1 β-GlcCer at 40 μg per well in a 12-well plate for 3 d. Data are presented as mean ± SD of duplicate (A–E) and triplicate (F and G) assays.

OT-II T cells were cultured with antigen-pulsed BMDCs in the presence or absence of plate-coated β-GlcCer. The antigen-specific secretion of IL-17 was significantly augmented by β-GlcCer treatment but not when Mincle$^{-/-}$ APCs were used (Fig. 4A). Antigen-specific proliferation and IFN-γ production were not further enhanced in this in vitro condition (Fig. S4). These results suggest that β-GlcCer acts through Mincle to promote antigen-specific T-cell responses on APCs.

To evaluate this function in vivo, mice were immunized with OVA, along with β-GlcCer or TDM as adjuvants, to induce delayed-type hypersensitivity responses. As assessed by footpad swelling, the β-GlcCer–induced delayed-type hypersensitivity response was comparable to that triggered by TDM (Fig. 4B). Furthermore, β-GlcCer induced the production of IFN-γ at the same level as did TDM in recall responses after ex vivo stimulation with OVA (Fig. 4C). Antigen-specific production of IL-17 was not detected in cells from both TDM- and β-GlcCer–treated mice. Collectively, these results indicate that β-GlcCer may function as an adjuvant to promote acquired immune responses.

Accumulation of Endogenous β-GlcCer Enhances Inflammatory Responses. We next examined the effect of endogenous β-GlcCer on immune responses in vivo. Mice in which GBA1 is mutated accumulate β-GlcCer and are used as a mouse model of Gaucher disease (32). Because homozygous mutation of the GBA1 gene results in neonatal lethality, we collected hematopoietic progenitor cell (HPC)-containing fetal liver (FL) cells from GBA1$^{-/-}$ fetuses and transferred them into irradiated WT CD45.1 congenic mice to establish hematopoietic-specific GBA1-deficient mice (GBA1$^{\Delta HPC}$ mice). Eight weeks posttransfer, peripheral lymphocytes and myeloid cells in the recipient mice were almost fully reconstituted by CD45.2$^+$ cells derived from GBA1-deficient mice. GBA1$^{\Delta HPC}$ mice showed no altered cellularity of their thymus, spleen, or lymph nodes, compared with control mice (Fig. S5).

We therefore assessed the role of endogenous β-GlcCer in inflammatory responses in these mice. Excessive or deregulated cell death induces transient infiltration of inflammatory cells despite the absence of infection. A model system with which to study this phenomenon involves whole-body irradiation of mice, which induces massive death of thymocytes and consequently elicits transient infiltration of neutrophils into the thymus (5) (Fig. 5A). WT and WT FL-transferred mice showed a significant infiltration of neutrophils after whole-body irradiation. The number of infiltrating neutrophils was further enhanced in GBA1$^{\Delta HPC}$ mice (Fig. 5B), although there was no difference in thymocyte death among these genotypes (Fig. 5C), thus implying that accumulation of β-GlcCer serves to promote inflammation induced by cell death. Notably, the average number of infiltrating cells was lower when Mincle was deleted on a GBA1-deficient background (GBA1/Mincle$^{\Delta HPC}$ mice), suggesting that accumulation of β-GlcCer exacerbates the inflammation induced by dead cells, and Mincle plays a major role in this process.

GBA1-Deficient DCs Enhance Acquired Immune Responses. To investigate the cell-intrinsic effects of β-GlcCer accumulation in vitro, we analyzed BMDCs from GBA1$^{\Delta HPC}$ mice. DCs derived from GBA1$^{\Delta HPC}$ mice (GBA1$^{-/-}$ DCs) contained increased levels of β-GlcCer compared with GBA1-sufficient WT mice (Fig. 6A). GBA1$^{-/-}$ DCs had higher expression levels of MHC class II, CD40, and CD86 compared with WT control. This augmentation was not observed in GBA1 × Mincle double-deficient (GBA1$^{-/-}$ × Mincle$^{-/-}$) DCs (Fig. 6B), although β-GlcCer accumulation still occurred regardless of Mincle expression (Fig. 6A). We then asked whether β-GlcCer released during cell culture can act as a paracrine factor to influence surrounding cells. When CD45.1$^+$ WT DCs were cocultured with CD45.2$^+$ GBA1-deficient DCs, the expression of costimulatory molecules on WT DCs was upregulated significantly (Fig. 6C). Thus, upon cell damage during
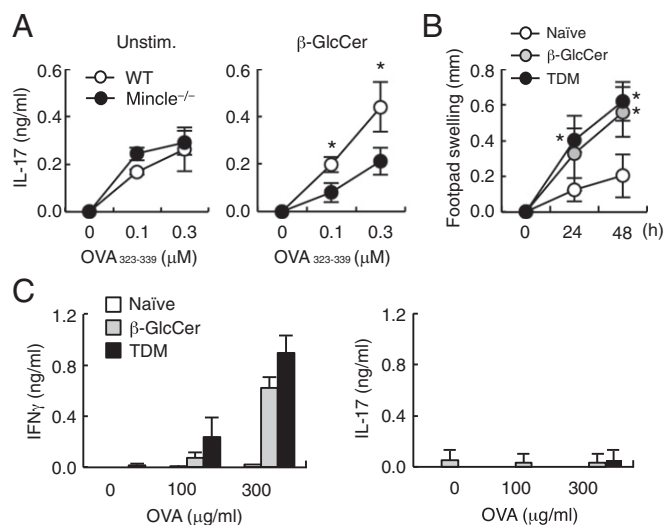

Fig. 4. β-GlcCer functions as an adjuvant to promote T-cell responses. (A) WT or Mincle$^{-/-}$ BMDCs were stimulated with 2 nmol per well of 24:1 β-GlcCer (β-GlcCer) or left unstimulated (Unstim.), and cocultured with OT-II CD4$^+$ T cells in the presence of OVA$_{323–339}$ peptide at the indicated concentrations. The concentration of IL-17 produced was determined by ELISA. *$P < 0.05$ versus WT mice. (B) WT mice were sensitized by OVA in oil-in-water emulsion of TDM or 24:1 β-GlcCer and challenged with heat-aggregated OVA 7 d later. Foot pad swelling was measured before and 24 and 48 h after challenge. Data are means ± SD of three mice per group. *$P < 0.05$ versus naïve mice. (C) Inguinal lymph node T cells were purified from mice 10 d after OVA challenge. Cells were stimulated with OVA protein and cytokine concentrations were determined by ELISA at day 4. Data are presented as mean ± SD of triplicate assays (A and C).

ing culture, GBA1-deficient cells can stimulate surrounding cells by releasing β-GlcCer.

We also introduced the Mincle transgene (Tg) onto the GBA1$^{-/-}$ background to assess the contribution of the β-GlcCer–Mincle axis to APC function. BMDCs overexpressing Mincle and β-GlcCer were pulsed with OVA peptides and cocultured with OT-II T cells. GBA1$^{-/-}$ BMDCs stimulated the production of IFN-γ by OT-II T cells, more so than did WT BMDCs (Fig. 6D). Furthermore, the immunostimulatory effect of GBA1$^{-/-}$ BMDCs was markedly enhanced by overexpression of Mincle (GBA1$^{-/-}$ × Mincle Tg BMDCs) (Fig. 6E) and was cancelled by the deletion of Mincle (GBA1$^{-/-}$ × Mincle$^{-/-}$ BMDCs) (Fig. 6F). Collectively, these in vitro results suggest that the accumulation of β-GlcCer enhances APC functions in a Mincle-dependent manner.

Finally, we evaluated the effect of accumulated β-GlcCer in APCs on triggering immune responses in vivo. WT mice were immunized with WT or GBA1$^{-/-}$ BMDCs that had been pulsed with OVA protein. Mice injected with OVA-pulsed DCs produce antigen-specific antibodies, but the average titers of anti-OVA IgG were higher for mice injected with GBA1-deficient DCs (Fig. S6). The efficiency of T-cell priming in these mice was evaluated by recall T-cell responses. Antigen-specific IFN-γ production was augmented in mice immunized with GBA1-deficient DCs in a Mincle-dependent manner (Fig. 6G). These results suggest that excessive β-GlcCer acts as an endogenous adjuvant to promote acquired immune responses through APC activation.

Discussion

In this study, we identified β-GlcCer as an endogenous ligand for Mincle. β-GlcCer is a common glycolipid present in most animals and the β-GlcCer–Mincle axis is the first example of a self-glycolipid–CLR pathway conserved in a wide-variety of mammalian species. In
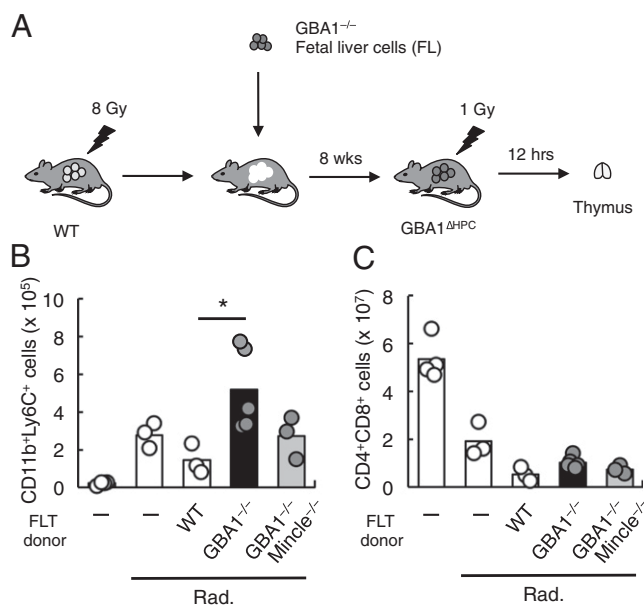
Fig. 5. GBA1 deficiency in hematopoietic cells results in increased inflammation. (*A*) Schematic procedure for the establishment of hematopoietic-specific GBA1-deficient mice (GBA1$^{\Delta HPC}$) and the dead cell-induced inflammation. (*B* and *C*) Absolute cell numbers of CD11b$^+$Ly6C$^+$ cells (*B*) and CD4$^+$CD8$^+$ cells (*C*) in the thymus from WT, GBA1$^{-/-}$ and GBA1$^{-/-}$ × Mincle$^{-/-}$ FL-transferred (FLT) mice 12 h after 1 Gy-irradiation (Rad.). Nontransferred mice (−) were also analyzed as controls. Four, three, three, five, and three mice were used, respectively, in each group. Data are representative of three experiments with similar results. *$P < 0.05$.

fact, β-GlcCer was recognized by Mincle derived from all mammalian species tested to date.

A common Mincle ligand signature structure has been predicted based on a number of identified ligands (6, 7, 33–35) in combination with the Mincle protein structure (9–12). A polar head consisting of glucose or mannose and a hydrophobic chain appear to be the minimum requirement for ligand activity. All six β-GlcCer species examined in this study satisfy these criteria as they harbor a polar glucose head and two acyl chains within the ceramide moiety. It remains unclear why the unsaturated β-GlcCer C24:1(15Z) possesses the most potent ligand activity, as the crystal structure of Mincle (9, 10, 12) suggested that the double bond of C24:1 is likely to be located away from the Mincle interacting site. Cocrystallization of Mincle protein and β-GlcCer C24:1 should clarify this issue.

The composition of β-GlcCer acyl chains (i.e., length and saturation) differs among tissues (18, 36). C24:1 is abundantly expressed in brain tissue (36, 37) and accumulates greatly in Gaucher disease patients (38). The pathophysiological role of Mincle in neural symptoms is a critical issue that remains to be clarified. As another example, epidermis has a unique GlcCer epidermoside, which is composed of a longer unsaturated ω-hydroxy FA that functions to maintain the epidermal permeability barrier (39, 40). Given that glycolipids with longer FA have potent activities (10, 11, 34, 35), epidermosides might be recognized by Mincle on dermal Mφ/DCs and thereby modulate immune responses in skin. Interestingly, Mincle is involved in the immune response against fungi that causes skin disease (41) through the recognition of its unique glycolipids (7, 42). It is tempting to speculate that both pathogen-derived and skin-derived glycolipids contribute to disease onset or progression. In line with this hypothesis, as caseation necrosis is a characteristic feature of tuberculosis (43), glycolipids derived from dead cells and mycobacteria might synergistically contribute to the pathogenicity of tuberculosis, although it warrants further extensive investigation.

The average concentration of β-GlcCer in sera is in the nanomolar range in healthy individuals; in patients and in GBA1-deficient mice, β-GlcCer levels are elevated (44, 45) (Fig. S7*A*). Furthermore, β-GlcCer synthesis is increased in cells that have sustained damage (16, 46). Thus, in damaged tissues, it is plausible that β-GlcCer can signal through Mincle in vivo particularly when β-GlcCer is present locally in a multivalent form. Alternatively, a subtle continuous recognition of a low-level ligand by activating receptors might counterbalance inhibitory receptors that are constantly recognizing normal self (47). Such a dynamic, balanced "resting state" may enable myeloid cells to respond rapidly when damage or stress occurs.

β-GlcCer is localized in endoplasmic reticulum/Golgi in healthy cells, whereas Mincle is expressed not only on the cell surface but also in intracellular compartments, such as endosomes or lysosomes (48). Thus, Mincle may encounter β-GlcCer intracellularly, particularly when the localization of β-GlcCer is dysregulated upon cell damage. The possible role of Mincle as an intracellular sensor that monitors lipid metabolism warrants further investigation.

Other proteins have been reported as potential CLR ligands. For example, we previously purified the nuclear protein spliceosome-associated protein (SAP)-130 as a Mincle-Ig–binding protein (5). However, the exact contribution of SAP-130 as a damage-associated molecular pattern cannot be addressed by conventional genetic approaches, as this protein is essential for RNA splicing, a fundamental process in all living cells. For the same reason, the precise contribution of F-actin as a Clec9a ligand (49, 50) is difficult to prove by gene-deletion approaches, because actin is an indispensable cytoskeletal protein. Some other CLRs recognize crystallized self-components that do not exist under normal conditions (51, 52). Collectively these results suggest that CLRs may sense aberrant localizations or forms of various vital cell components as signals of damage. Further understanding of the principles of self-recognition via CLRs will require the structural analysis of various CLR-ligand complexes (53).

β-GlcCer has also been reported to be an activator of NKT cells (46, 54). However, two recent reports proposed that the activator might be α-GlcCer, as the activity was not influenced by treatment with β-glucosidase (55, 56). In contrast, Mincle ligand activity was eliminated by β-glucosidase (GBA1) treatment (Fig. S7 *B* and *C*), supporting our conclusion that β-GlcCer is a ligand for Mincle.

Exogenous administration of β-GlcCer has been reported to promote tumor regression by inducing NKT activation (57–59). Alternatively, our study suggests that this effect may derive from the adjuvant activity of β-GlcCer through Mincle on APCs. The application of endogenous components as adjuvants for T-cell activation could thus be beneficial for vaccination against infectious diseases and cancer. Notably, β-GlcCer did not induce granuloma formation (Fig. S7*D*), implying that β-GlcCer and its analogs may be safer adjuvant candidates with reduced adverse effects.

Mincle ligands have been reported to induce Th1 or Th17 or both Th1/Th17 responses (7, 60–63). Although the precise molecular mechanisms underlying different Th responses via the same CLRs are presently unknown, the intensity of signaling through ITAMs may determine the type of responses (63–66). Indeed, strong Mincle signaling delivered through plate-coated purified β-GlcCer preferentially induced Th17 responses. In addition, the different stimulus strength during T-cell priming is reported to alter Th orientation (67), which may explain the apparent contradictory results between in vitro vs. in vivo in this study.

Our current identification and analysis of the β-GlcCer–Mincle axis provides additional information regarding pathogenesis of Gaucher disease. However, all symptoms cannot be fully explained by this axis. For example, the neonatal lethality of GBA1$^{-/-}$ mice, which is mainly because of a keratinocyte disorder (68, 69), was not rescued on a Mincle-deficient background. Additionally, FL-derived GM-CSF myeloid cells from GBA1$^{-/-}$ mice displayed an enlarged cell size much like Gaucher cells, and this was observed
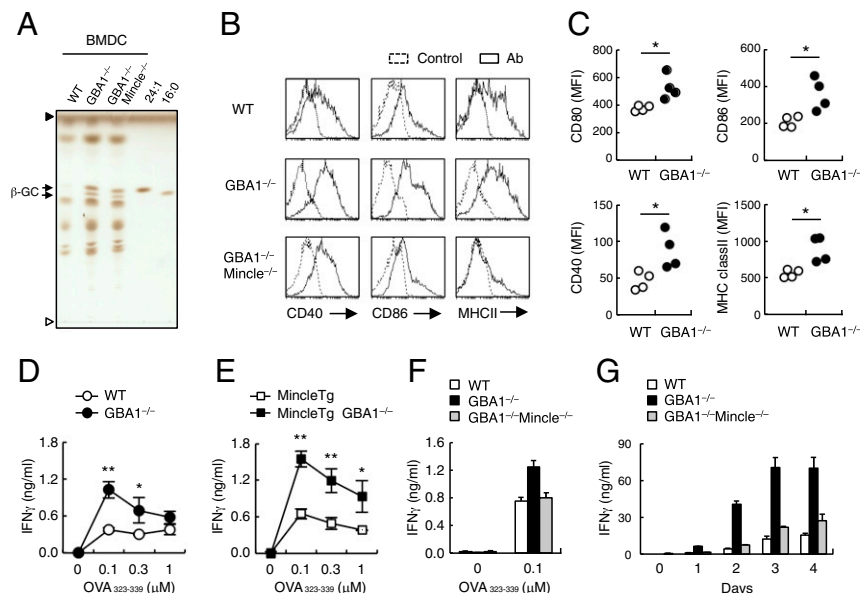
Fig. 6. GBA1-deficient BMDCs promote acquired immune responses. (*A*) Lipid extract from BMDCs derived from BM cells of WT, GBA1$^{-/-}$ and GBA1$^{-/-}$ × Mincle$^{-/-}$ FL-transferred mice were analyzed by HPTLC. Synthetic β-GlcCer (24:1 and 16:0) were used as controls. Open and closed arrowheads denote the origin and solvent fronts, respectively. (*B*) Surface expression levels of CD40, CD86, and MHC class II on BMDCs after 12 d culture of BM cells in the presence of GM-CSF were analyzed by flow cytometry. Dotted lines represent unstained controls. (*C*) CD45.1$^+$ WT BM cells were cocultured with CD45.2$^+$ WT or GBA1$^{-/-}$ BM cells during the induction of BMDCs. After 18 d, surface expression levels of CD80, CD86, CD40 and MHC class II of CD45.1$^+$ cells were analyzed by flow cytometry. Data are presented as mean fluorescent intensities (MFIs) and each symbol represents individual mice. (*D–F*) IFN-γ production by OT-II T cells cocultured with OVA peptide (OVA$_{323-339}$)-pulsed BMDCs from WT or GBA1$^{-/-}$ (*D*), Mincle Tg or Mincle Tg × GBA1$^{-/-}$ (*E*), WT, GBA1$^{-/-}$ or GBA1$^{-/-}$ × Mincle$^{-/-}$ mice (*F*) was determined by ELISA. (*G*) WT mice were sensitized by OVA-pulsed BMDCs from WT, GBA1$^{-/-}$ and GBA1$^{-/-}$ × Mincle$^{-/-}$ mice and challenged with heat-aggregated OVA 8 d later. Splenocytes were stimulated with 100 μg/mL of OVA protein 7 d after challenge. Concentrations of IFN-γ were determined by ELISA at the indicated days after stimulation. Data are presented as mean ± SD of triplicate assays (*D–G*). *$P < 0.05$. **$P < 0.01$.

regardless of Mincle expression. However, the β-GlcCer–Mincle axis may explain the inflammatory-prone phenotype, one of the important features of Gaucher disease. Another central characteristic of this disorder is neurodegeneration (70), raising the possibility that Mincle expressed on microglia (71) contributes to this pathology, as the most active β-GlcCer species C24:1 is abundantly expressed in brain (36, 37). Because microglia are not replaced by FL transfer experiments, conditional deletion of GBA1 and Mincle will be needed to address the role of Mincle in the CNS and this is now under investigation.

In addition to Gaucher disease, GBA1 mutation is genetically correlated with Parkinson's disease (72). It has been hypothesized that this results from the ability of β-GlcCer to promote neuro-toxic amyloid formation (73, 74). As we have now identified β-GlcCer as a Mincle ligand, the role of Mincle in these processes presents an intriguing issue to be addressed for the understanding of this severe progressive disease.

In conclusion, based on our work and in combination with other recent evidence, we propose here that Mincle may sense "damage" derived from self and nonself by recognizing "unfamiliar" glycolipids that are not present in the extracellular milieu under normal, healthy conditions.

Materials and Methods

Mice. Mincle-deficient mice (42) were backcrossed for at least nine generations with C57BL/6. FcRγ-deficient mice were developed on a C57BL/6 background, and were provided by T. Saito, RIKEN, Yokohama, Japan (75). CARD9-deficient mice were provided by H. Hara, Kagoshima University, Kagoshima, Japan (76). GBA1-deficient mice (32) were purchased from the Jackson Laboratory. Mincle Tg mice were previously described (77). GBA1$^{\Delta HPC}$ mice were established as described in Fig. 5*A* and *SI Materials and Methods*. All mice were maintained in a filtered-air laminar-flow enclosure and given standard laboratory food and water ad libitum. All animal protocols were approved by the committee of Ethics on Animal Experiments, Faculty of Medical Sciences, Kyushu University.

Reagents. Synthetic β-GlcCer [d18:1/C24:1(15Z), C18:0, C16:0, C12:0] and tre-halose dibehenate (TDB) were purchased from Avanti Polar Lipids. TDM was purchased from Sigma-Aldrich. LacCer was purchased from Nagara Science. Ceramide was purchased from Katayama Chemical Industries. β-GalCer was purchased from Matreya. D-PDMP was purchased from Cayman Chemical. Recombinant glucosylceramidase (rGBA1) was purchased from R&D.

Cells. The 2B4-NFAT-GFP reporter cells expressing Mincle, MCL, Dectin-2, or DCAR were prepared as previously described (5, 7, 62). HEK293-based NF-κB reporter cells expressing mMincle were obtained from InvivoGen. These reporter cells express an NF-κB-inducible secreted embryonic alkaline phosphatase (SEAP) reporter gene. BMDCs were prepared as previously described (7). The methods by which these cells were stimulated in in vitro assay are described in *SI Materials and Methods*.

Purification of β-GlcCer. The 2B4-NFAT-GFP or HEK293-based NF-κB reporter cells were cultured for 48 h without FBS to induce cell death. Lipid components from culture supernatant of dead cells were extracted with chloroform/methanol (2:1, vol/vol). These lipid extracts were separated by normal-phase HPLC using an Inertsil, SIL, 100A, 5-μm (250 × 7.6 mm) column, a Jasco PU-2086 Plus Interlligent HPLC pump, and UV-2075 Plus UV detector. A stepwise elution was performed with chloroform/methanol (9:1, vol/vol) for 10 min followed by methanol for 20 min at a flow rate of 2.7 mL/min. After HPLC separation, active fraction was further separated using HPTLC plates pre-coated with silica gel 60 (Merck). The mobile phase was chloroform/methanol/water (65:25:4, vol/vol/vol).

ESI-MS Analysis Using a Q-Orbitrap-MS. Lipid fractions were dissolved in 5 mM ammonium acetate (wt/vol) in methanol/water (95:5, vol/vol) (50 μg/mL). The flow injection analysis was performed using a Dinex Ultimate 3000 RSLC system (Thermo Fisher Scientific) coupled with a Q Exactive, a high-performance benchtop Q-Orbitrap-MS, fitted with an electrospray ionizaition (ESI) ion source (Thermo Fisher Scientific). The flow injection conditions were as follows: mobile phase, 5 mM ammonium acetate in methanol/water (95:5, vol/vol); flow rate, 0.2 mL/min; injection volume, 2 μL; and run time, 2 min. Individual lipid molecular species ware identified by a full-scanning MS/data-dependent MS^2 (dd-MS^2) analysis. The ionization conditions were as follows: ionization mode,

positive; sheath gas flow rate, 40 arb; auxiliary (AUX) gas flow rate, 10 arb; spray voltage 3,500 V; capillary temperature, 350 °C; S-lens level, 50; and heater temperature, 300 °C. The experimental conditions for full-scanning MS were as follows: resolving power, 70,000; automatic gain control (AGC) target, 1×10^6; trap fill time, 200 ms; and scan range m/z 400–3,000. The experimental conditions for dd-MS^2 were as follows: resolving power, 17,500; AGC target, 5×10^4; and trap fill time, 80 ms; isolation width, $\pm$ 0.6 Da; fixed first mass, m/z 80; and stepped normalized collision energy, 10, 20, 30 eV. The intensity threshold of precursor ions for dd-MS^2 analysis, the apex trigger, and the dynamic exclusion were set to 5,000, 2–4 s, and 2 s, respectively. The ESI-MS analyses were controlled using the software Xcalibur 3.0.63 (Thermo Fisher Scientific).

NMR. ^{1}H- and ^{13}C-NMR spectra were recorded on a Varian INOVA 600 spectrometer. The operating conditions were as follows: ^{1}H: 600 MHz, 300 K, CDCl$_3$/CD$_3$OD/D$_2$O (60:35:5, vol/vol/vol). ^{13}C: 125 MHz, 300 K, CDCl$_3$/CD$_3$OD/D$_2$O (60:35:5, vol/vol/vol). ^{1}H chemical shifts were determined by 2D-NMR (COSY, TOCSY, NOESY, HMGC, HMBC). Geometrical isomerism of double bond in the FA side chain was determined by ^{13}C chemical shifts of allylic position.

In Vitro Mincle Binding Assay. Mincle-Ig protein, the C terminus of the extracellular domain of Mincle fused to the N terminus of human IgG1 Fc region (hIgG1), was prepared as described previously (5). For the in vitro binding assay, 3 μg/mL of hIgG1-Fc (Ig) and Mincle-Ig diluted in binding buffer (20 mM Tris·HCl, 150 mM NaCl, 1 mM CaCl$_2$, 2 mM MgCl$_2$, pH 7.0) were incubated with plate-coated glycolipids. Anti-hIgG-HRP was used for the detection of bound protein by the addition of colorimetric substrate. Peroxidase activity was measured by spectrophotometer.

Delayed-Type Hypersensivity. Mice were sensitized by subcutaneous injection with 200 μg of OVA in oil-in-water emulsion [mineral oil/Tween-80/PBS (9:1:90, vol/vol/vol)] of 100 μg β-GlcCer or TDM as previously described (78). At day 7, mice were challenged by injecting 200 μg of heat-aggregated OVA (70 °C, 1 h) in 20 μL of PBS into both footpads. Footpad swelling was measured using a vernier caliper and calculated as (footpad thickness after challenge) – (foodpad thickness before challenge). For in vitro restimulation analysis, inguinal lymph nodes were collected 7–10 d after challenge. B cells were depleted using MACS beads (Miltenyi Biotec) and then stimulated with OVA protein for the indicated periods.

Immunization with OVA-Pulsed BMDCs. For OVA peptide presentation on MHC class II, BMDCs were cultured in the presence of 100 μg/mL OVA for 1 d. BMDCs were then harvested and resuspended in PBS at a concentration of 1×10^6 cells/mL Mice were sensitized by subcutaneous injection of 2×10^5 cells/200 μL OVA-pulsed BMDCs. At day 7 or 8, mice were challenged by injecting 200 μg of heat-aggregated OVA (70 °C, 1 h) in 20 μL PBS into both footpads. For in vitro restimulation analysis, splenocytes were collected 7–11 d after challenge and then stimulated with OVA protein for the indicated periods.

Dead Cell-Induced Inflammation. Mice were irradiated with γ-rays (1 Gy). Absolute number and cellularity of thymocytes were analyzed at 12 h after irradiation. The number of CD11b$^+$Ly6C$^+$ infiltrating cells and CD4$^+$CD8$^+$ double-positive thymocytes were analyzed by flow cytometry.

Statistics. An unpaired two-tailed Student's t test was used for all statistical analyses.

1. Miyake K, Kaisho T (2014) Homeostatic inflammation in innate immunity. *Curr Opin Immunol* 30:85–90.
2. Sancho D, Reis e Sousa C (2013) Sensing of cell death by myeloid C-type lectin receptors. *Curr Opin Immunol* 25:46–52.
3. Geddes K, Magalhães JG, Girardin SE (2009) Unleashing the therapeutic potential of NOD-like receptors. *Nat Rev Drug Discov* 8:465–479.
4. Roers A, Hiller B, Hornung V (2016) Recognition of endogenous nucleic acids by the innate immune system. *Immunity* 44:739–754.
5. Yamasaki S, et al. (2008) Mincle is an ITAM-coupled activating receptor that senses damaged cells. *Nat Immunol* 9:1179–1188.
6. Ishikawa E, et al. (2009) Direct recognition of the mycobacterial glycolipid, trehalose dimycolate, by C-type lectin Mincle. *J Exp Med* 206:2879–2888.
7. Ishikawa T, et al. (2013) Identification of distinct ligands for the C-type lectin receptors Mincle and Dectin-2 in the pathogenic fungus *Malassezia*. *Cell Host Microbe* 13:477–488.
8. Hattori Y, et al. (2014) Glycerol monomycolate is a novel ligand for the human, but not mouse macrophage inducible C-type lectin, Mincle. *J Biol Chem* 289:15405–15412.
9. Feinberg H, et al. (2013) Mechanism for recognition of an unusual mycobacterial glycolipid by the macrophage receptor mincle. *J Biol Chem* 288:28457–28465.
10. Furukawa A, et al. (2013) Structural analysis for glycolipid recognition by the C-type lectins Mincle and MCL. *Proc Natl Acad Sci USA* 110:17438–17443.
11. Jégouzo SA, et al. (2014) Defining the conformation of human Mincle that interacts with mycobacterial trehalose dimycolate. *Glycobiology* 24:1291–1300.
12. Feinberg H, et al. (2016) Binding sites for acylated trehalose analogs of glycolipid ligands on an extended carbohydrate-recognition domain of the macrophage receptor mincle. *J Biol Chem* 291:21222–21233.
13. D'Angelo G, et al. (2007) Glycosphingolipid synthesis requires FAPP2 transfer of glucosylceramide. *Nature* 449:62–67.
14. Halter D, et al. (2007) Pre- and post-Golgi translocation of glucosylceramide in glycosphingolipid synthesis. *J Cell Biol* 179:101–115.
15. Yamaji T, Hanada K (2015) Sphingolipid metabolism and interorganellar transport: Localization of sphingolipid enzymes and lipid transfer proteins. *Traffic* 16:101–122.
16. Memon RA, et al. (1999) Regulation of glycosphingolipid metabolism in liver during the acute phase response. *J Biol Chem* 274:19707–19713.
17. Reczek D, et al. (2007) LIMP-2 is a receptor for lysosomal mannose-6-phosphate-independent targeting of β-glucocerebrosidase. *Cell* 131:770–783.
18. Ishibashi Y, Kohyama-Koganeya A, Hirabayashi Y (2013) New insights on glucosylated lipids: Metabolism and functions. *Biochim Biophys Acta* 1831:1475–1485.
19. Hruska KS, LaMarca ME, Scott CR, Sidransky E (2008) Gaucher disease: Mutation and polymorphism spectrum in the glucocerebrosidase gene (GBA). *Hum Mutat* 29:567–583.
20. Mizukami H, et al. (2002) Systemic inflammation in glucocerebrosidase-deficient mice with minimal glucosylceramide storage. *J Clin Invest* 109:1215–1221.
21. Enquist IB, et al. (2007) Murine models of acute neuronopathic Gaucher disease. *Proc Natl Acad Sci USA* 104:17483–17488.
22. Vitner EB, Farfel-Becker T, Eilam R, Biton I, Futerman AH (2012) Contribution of brain inflammation to neuronal cell death in neuronopathic forms of Gaucher's disease. *Brain* 135:1724–1735.
23. Mistry PK, et al. (2010) Glucocerebrosidase gene-deficient mouse recapitulates Gaucher disease displaying cellular and molecular dysregulation beyond the macrophage. *Proc Natl Acad Sci USA* 107:19473–19478.
24. Gervas-Arruga J, et al. (2015) The influence of genetic variability and proinflammatory status on the development of bone disease in patients with Gaucher disease. *PLoS One* 10:e0126153.
25. Yamada T, et al. (2013) Development of a lipid profiling system using reverse-phase liquid chromatography coupled to high-resolution mass spectrometry with rapid polarity switching and an automated lipid identification software. *J Chromatogr A* 1292:211–218.
26. Hsu FF, Turk J, Stewart ME, Downing DT (2002) Structural studies on ceramides as lithiated adducts by low energy collisional-activated dissociation tandem mass spectrometry with electrospray ionization. *J Am Soc Mass Spectrom* 13:680–695.
27. Wishart DS, et al. (2013) HMDB 3.0—The human metabolome database in 2013. *Nucleic Acids Res* 41:D801–D807.
28. Koerner TA, Jr, Cary LW, Li SC, Li YT (1979) Carbon 13 NMR spectroscopy of a cerebroside. Proof of the β-pyranosyl structure of D-glucosylceramide. *J Biol Chem* 254:2326–2328.
29. Hamanaka S, Asagami C, Suzuki M, Inagaki F, Suzuki A (1989) Structure determination of glucosyl β1-N-(ω-O-linoleoyl)-acylsphingosines of human epidermis. *J Biochem* 105:684–690.
30. Haan JWD, Vandeven LJ (1973) Configurations and conformations in acyclic, unsaturated-hydrocarbons. A ^{13}C NMR study. *Org Magn Resonance* 5:147–153.
31. Felding-Habermann B, et al. (1990) A ceramide analogue inhibits T cell proliferative response through inhibition of glycosphingolipid synthesis and enhancement of N,N-dimethylsphingosine synthesis. *Biochemistry* 29:6314–6322.
32. Tybulewicz VL, et al. (1992) Animal model of Gaucher's disease from targeted disruption of the mouse glucocerebrosidase gene. *Nature* 357:407–410.
33. van der Peet PL, Gunawan C, Torigoe S, Yamasaki S, Williams SJ (2015) Corynomycolic acid-containing glycolipids signal through the pattern recognition receptor Mincle. *Chem Commun (Camb)* 51:5100–5103.
34. Richardson MB, Torigoe S, Yamasaki S, Williams SJ (2015) *Mycobacterium tuberculosis* β-gentiobiosyl diacylglycerides signal through the pattern recognition receptor Mincle: Total synthesis and structure activity relationships. *Chem Commun (Camb)* 51:15027–15030.
35. Stocker BL, Khan AA, Chee SH, Kamena F, Timmer MS (2014) On one leg: Trehalose monoesters activate macrophages in a Mincle-dependant manner. *ChemBioChem* 15:382–388.
36. Laviad EL, et al. (2008) Characterization of ceramide synthase 2: Tissue distribution, substrate specificity, and inhibition by sphingosine 1-phosphate. *J Biol Chem* 283:5677–5684.
37. Boutin M, Sun Y, Shacka JJ, Auray-Blais C (2016) Tandem mass spectrometry multiplex analysis of glucosylceramide and galactosylceramide isoforms in brain tissues at different stages of Parkinson disease. *Anal Chem* 88:1856–1863.

38. Burrow TA, et al. (2015) CNS, lung, and lymph node involvement in Gaucher disease type 3 after 11 years of therapy: Clinical, histopathologic, and biochemical findings. *Mol Genet Metab* 114:233–241.

39. Jennemann R, et al. (2007) Integrity and barrier function of the epidermis critically depend on glucosylceramide synthesis. *J Biol Chem* 282:3083–3094.

40. Hamanaka S, et al. (2002) Human epidermal glucosylceramides are major precursors of stratum corneum ceramides. *J Invest Dermatol* 119:416–423.

41. Ashbee HR (2006) Recent developments in the immunology and biology of *Malassezia* species. *FEMS Immunol Med Microbiol* 47:14–23.

42. Yamasaki S, et al. (2009) C-type lectin Mincle is an activating receptor for pathogenic fungus, *Malassezia*. *Proc Natl Acad Sci USA* 106:1897–1902.

43. Adams DO (1976) The granulomatous inflammatory response. A review. *Am J Pathol* 84:164–192.

44. Dawson G, Oh JY (1977) Blood glucosylceramide levels in Gaucher's disease and its distribution amongst lipoprotein fractions. *Clin Chim Acta* 75:149–153.

45. Groener JE, Poorthuis BJ, Kuiper S, Hollak CE, Aerts JM (2008) Plasma glucosylceramide and ceramide in type 1 Gaucher disease patients: Correlations with disease severity and response to therapeutic intervention. *Biochim Biophys Acta* 1781:72–78.

46. Brennan PJ, et al. (2011) Invariant natural killer T cells recognize lipid self antigen induced by microbial danger signals. *Nat Immunol* 12:1202–1211.

47. Ravetch JV, Lanier LL (2000) Immune inhibitory receptors. *Science* 290:84–89.

48. Ostrop J, et al. (2015) Contribution of MINCLE-SYK signaling to activation of primary human APCs by mycobacterial cord factor and the novel adjuvant TDB. *J Immunol* 195:2417–2428.

49. Ahrens S, et al. (2012) F-actin is an evolutionarily conserved damage-associated molecular pattern recognized by DNGR-1, a receptor for dead cells. *Immunity* 36:635–645.

50. Zhang JG, et al. (2012) The dendritic cell receptor Clec9A binds damaged cells via exposed actin filaments. *Immunity* 36:646–657.

51. Kiyotake R, et al. (2015) Human mincle binds to cholesterol crystals and triggers innate immune responses. *J Biol Chem* 290:25322–25332.

52. Neumann K, et al. (2014) Clec12a is an inhibitory receptor for uric acid crystals that regulates inflammation in response to cell death. *Immunity* 40:389–399.

53. Hanč P, et al. (2015) Structure of the complex of F-actin and DNGR-1, a C-type lectin receptor involved in dendritic cell cross-presentation of dead cell-associated antigens. *Immunity* 42:839–849.

54. Zigmond E, et al. (2007) β-glucosylceramide: A novel method for enhancement of natural killer T lymphoycte plasticity in murine models of immune-mediated disorders. *Gut* 56:82–89.

55. Kain L, et al. (2014) The identification of the endogenous ligands of natural killer T cells reveals the presence of mammalian α-linked glycosylceramides. *Immunity* 41:543–554.

56. Brennan PJ, et al. (2014) Activation of iNKT cells by a distinct constituent of the endogenous glucosylceramide fraction. *Proc Natl Acad Sci USA* 111:13433–13438.

57. Inafuku M, et al. (2012) Beta-glucosylceramide administration (i.p.) activates natural killer T cells in vivo and prevents tumor metastasis in mice. *Lipids* 47:581–591.

58. Oku H, et al. (2009) Tumor specific cytotoxicity of β-glucosylceramide: structure-cytotoxicity relationship and anti-tumor activity in vivo. *Cancer Chemother Pharmacol* 64:485–496.

59. Symolon H, Schmelz EM, Dillehay DL, Merrill AH, Jr (2004) Dietary soy sphingolipids suppress tumorigenesis and gene expression in 1,2-dimethylhydrazine-treated CF1 mice and ApcMin/+ mice. *J Nutr* 134:1157–1161.

60. Werninghaus K, et al. (2009) Adjuvanticity of a synthetic cord factor analogue for subunit *Mycobacterium tuberculosis* vaccination requires FcRγ-Syk-Card9-dependent innate immune activation. *J Exp Med* 206:89–97.

61. Schoenen H, et al. (2010) Cutting edge: Mincle is essential for recognition and adjuvanticity of the mycobacterial cord factor and its synthetic analog trehalose-dibehenate. *J Immunol* 184:2756–2760.

62. Miyake Y, et al. (2013) C-type lectin MCL is an FcRγ-coupled receptor that mediates the adjuvanticity of mycobacterial cord factor. *Immunity* 38:1050–1062.

63. Geijtenbeek TB, Gringhuis SI (2016) C-type lectin receptors in the control of T helper cell differentiation. *Nat Rev Immunol* 16:433–448.

64. Davidsen J, et al. (2005) Characterization of cationic liposomes based on dimethyldioctadecylammonium and synthetic cord factor from *M. tuberculosis* (trehalose 6,6′-dibehenate)-a novel adjuvant inducing both strong CMI and antibody responses. *Biochim Biophys Acta* 1718:22–31.

65. Iezzi G, et al. (2009) CD40-CD40L cross-talk integrates strong antigenic signals and microbial stimuli to induce development of IL-17-producing CD4+ T cells. *Proc Natl Acad Sci USA* 106:876–881.

66. Huber A, et al. (2016) Trehalose diester glycolipids are superior to the monoesters in binding to Mincle, activation of macrophages in vitro and adjuvant activity in vivo. *Innate Immun* 22:405–418.

67. Yamane H, Paul WE (2012) Cytokines of the γc family control CD4+ T cell differentiation and function. *Nat Immunol* 13:1037–1044.

68. Sidransky E, Sherer DM, Ginns EI (1992) Gaucher disease in the neonate: A distinct Gaucher phenotype is analogous to a mouse model created by targeted disruption of the glucocerebrosidase gene. *Pediatr Res* 32:494–498.

69. Holleran WM, et al. (1994) Consequences of β-glucocerebrosidase deficiency in epidermis. Ultrastructure and permeability barrier alterations in Gaucher disease. *J Clin Invest* 93:1756–1764.

70. Cabrera-Salazar MA, et al. (2012) Systemic delivery of a glucosylceramide synthase inhibitor reduces CNS substrates and increases lifespan in a mouse model of type 2 Gaucher disease. *PLoS One* 7:e43310.

71. McKimmie CS, Roy D, Forster T, Fazakerley JK (2006) Innate immune response gene expression profiles of N9 microglia are pathogen-type specific. *J Neuroimmunol* 175:128–141.

72. Aharon-Peretz J, Rosenbaum H, Gershoni-Baruch R (2004) Mutations in the glucocerebrosidase gene and Parkinson's disease in Ashkenazi Jews. *N Engl J Med* 351:1972–1977.

73. Mazzulli JR, et al. (2011) Gaucher disease glucocerebrosidase and α-synuclein form a bidirectional pathogenic loop in synucleinopathies. *Cell* 146:37–52.

74. Yap TL, et al. (2011) α-synuclein interacts with Glucocerebrosidase providing a molecular link between Parkinson and Gaucher diseases. *J Biol Chem* 286:28080–28088.

75. Park SY, et al. (1998) Resistance of Fc receptor-deficient mice to fatal glomerulonephritis. *J Clin Invest* 102:1229–1238.

76. Hara H, et al. (2007) The adaptor protein CARD9 is essential for the activation of myeloid cells through ITAM-associated and Toll-like receptors. *Nat Immunol* 8:619–629.

77. Miyake Y, Masatsugu OH, Yamasaki S (2015) C-type lectin receptor MCL facilitates Mincle expression and signaling through complex formation. *J Immunol* 194:5366–5374.

78. Numata F, et al. (1985) Lethal and adjuvant activities of cord factor (trehalose-6,6′-dimycolate) and synthetic analogs in mice. *Chem Pharm Bull (Tokyo)* 33:4544–4555.